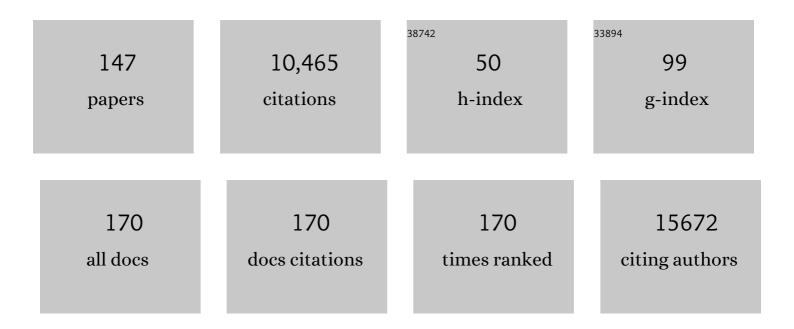
Chong Rae Park

List of Publications by Year in descending order

Source: https://exaly.com/author-pdf/6921951/publications.pdf Version: 2024-02-01



#	Article	IF	CITATIONS
1	Concentration-driven polymorphic mesocrystal and morphosynthetic transformation toward omni-adsorbent with the widest range of pores. Chemical Engineering Journal, 2022, 433, 133871.	12.7	2
2	Highly Integrated, Wearable Carbonâ€Nanotube‥arnâ€Based Thermoelectric Generators Achieved by Selective Inkjetâ€Printed Chemical Doping. Advanced Energy Materials, 2022, 12, .	19.5	19
3	High-Performance Thermoelectric Fabric Based on a Stitched Carbon Nanotube Fiber. ACS Applied Materials & Interfaces, 2021, 13, 6257-6264.	8.0	43
4	High-throughput thermal plasma synthesis of Fe _{<i>x</i>} Co _{1â^'<i>x</i>} nano-chained particles with unusually high permeability and their electromagnetic wave absorption properties at high frequency (1–26 GHz). Nanoscale, 2021, 13, 12004-12016.	5.6	10
5	Surface energy modification of graphene oxide film by silanization co-functionalized with fluorine to maximize the moisture barrier property. Synthetic Metals, 2021, 277, 116770.	3.9	6
6	Nanostructured Inorganic Chalcogenide-Carbon Nanotube Yarn having a High Thermoelectric Power Factor at Low Temperature. ACS Nano, 2021, 15, 13118-13128.	14.6	24
7	One step "growth to spinning―of biaxially multilayered CNT web electrode for long cycling Li–O2 batteries. Carbon, 2021, 182, 318-326.	10.3	7
8	Bifunctional Graphene Oxide Hole-Transporting and Barrier Layers for Transparent Bifacial Flexible Perovskite Solar Cells. ACS Applied Energy Materials, 2021, 4, 8824-8831.	5.1	8
9	A New Class of Carbon Nanostructures for Highâ€Performance Electroâ€Magnetic and â€Chemical Barriers. Advanced Science, 2021, 8, e2102718.	11.2	5
10	High-Performance, Wearable Thermoelectric Generator Based on a Highly Aligned Carbon Nanotube Sheet. ACS Applied Energy Materials, 2020, 3, 1199-1206.	5.1	43
11	Enhancing the cycle stability of Li–O ₂ batteries <i>via</i> functionalized carbon nanotube-based electrodes. Journal of Materials Chemistry A, 2020, 8, 4263-4273.	10.3	15
12	Electrostabilized homogeneous dispersion of boron nitride nanotubes in wide-range of solvents achieved by surface polarity modulation through pyridine attachment. Nano Research, 2020, 13, 344-352.	10.4	10
13	Band gap engineering of graphene oxide for ultrasensitive NO2 gas sensing. Carbon, 2020, 159, 175-184.	10.3	52
14	Molecular engineering of hydrocarbon membrane to substitute perfluorinated sulfonic acid membrane for proton exchange membrane fuel cell operation. Materials Today Energy, 2020, 17, 100483.	4.7	20
15	Lithium Ion Batteries: Atomicâ€Distributed Coordination State of Metalâ€Phenolic Compounds Enabled Low Temperature Graphitization for Highâ€Performance Multioriented Graphite Anode (Small 33/2020). Small, 2020, 16, 2070182.	10.0	1
16	High-Energy Density Li–O ₂ Battery with a Polymer Electrolyte-Coated CNT Electrode via the Layer-by-Layer Method. ACS Applied Materials & Interfaces, 2020, 12, 17385-17395.	8.0	21
17	Atomicâ€Distributed Coordination State of Metalâ€Phenolic Compounds Enabled Low Temperature Graphitization for Highâ€Performance Multioriented Graphite Anode. Small, 2020, 16, e2003104.	10.0	16
18	Function-regeneration of non-porous hydrolyzed-MOF-derived materials. Nano Research, 2019, 12, 1921-1930.	10.4	14

#	Article	IF	CITATIONS
19	Direct spinning and densification method for high-performance carbon nanotube fibers. Nature Communications, 2019, 10, 2962.	12.8	126
20	Enhanced gas barrier property of stacking-controlled reduced graphene oxide films for encapsulation of polymer solar cells. Carbon, 2019, 150, 275-283.	10.3	18
21	Revisiting the Role of Graphene Quantum Dots in Ternary Organic Solar Cells: Insights into the Nanostructure Reconstruction and Effective Förster Resonance Energy Transfer. ACS Applied Energy Materials, 2019, 2, 8826-8835.	5.1	17
22	Demonstration of the nanosize effect of carbon nanomaterials on the dehydrogenation temperature of ammonia borane. Nanoscale Advances, 2019, 1, 4697-4703.	4.6	13
23	Versatile reorganization of metal-polyphenol coordination on CNTs for dispersion, assembly, and transformation. Carbon, 2019, 144, 402-409.	10.3	10
24	Characteristics tuning of graphene-oxide-based-graphene to various end-uses. Energy Storage Materials, 2018, 14, 8-21.	18.0	43
25	Rational Design of Nanostructured Functional Interlayer/Separator for Advanced Li–S Batteries. Advanced Functional Materials, 2018, 28, 1707411.	14.9	272
26	How can we make carbon nanotube yarn stronger?. Composites Science and Technology, 2018, 166, 95-108.	7.8	66
27	Extremely Vivid, Highly Transparent, and Ultrathin Quantum Dot Lightâ€Emitting Diodes. Advanced Materials, 2018, 30, 1703279.	21.0	157
28	Macroscopically interconnected hierarchically porous carbon monolith by metal-phenolic coordination as an sorbent for multi-scale molecules. Carbon, 2018, 126, 190-196.	10.3	19
29	Rational Design of 1D Partially Graphitized N-Doped Hierarchical Porous Carbon with Uniaxially Packed Carbon Nanotubes for High-Performance Lithium-Ion Batteries. ACS Nano, 2018, 12, 11106-11119.	14.6	33
30	High-performance thermoelectric bracelet based on carbon nanotube ink printed directly onto a flexible cable. Journal of Materials Chemistry A, 2018, 6, 19727-19734.	10.3	44
31	Revisit to the correlation of surface characteristic nature with performance of N-enriched carbon-based supercapacitor. Carbon, 2018, 140, 68-76.	10.3	15
32	Highly Enhanced Cycleability from High Crystalline Biaxially Aligned CNT Web for Li-Air Cathode Applications. ECS Meeting Abstracts, 2018, , .	0.0	1
33	Metal–Phenolic Carbon Nanocomposites for Robust and Flexible Energyâ€Storage Devices. ChemSusChem, 2017, 10, 1675-1682.	6.8	30
34	Secondary Interactions of Graphene Oxide on Liquid Crystal Formation and Stability. Particle and Particle Systems Characterization, 2017, 34, 1600383.	2.3	12
35	Metal-Phenolic Carbon Nanocomposites for Robust and Flexible Energy-Storage Devices. ChemSusChem, 2017, 10, 1644-1644.	6.8	4
36	Crucial Role of Oxidation Debris of Carbon Nanotubes in Subsequent End-Use Applications of Carbon Nanotubes. ACS Applied Materials & Interfaces, 2017, 9, 17552-17564.	8.0	10

#	Article	IF	CITATIONS
37	Influence of the physicochemical characteristics of reduced graphene oxides on the gas permeability of the barrier films for organic electronics. Chemical Communications, 2017, 53, 6573-6576.	4.1	6
38	High-modulus and strength carbon nanotube fibers using molecular cross-linking. Carbon, 2017, 118, 413-421.	10.3	83
39	Highly dispersible edge-selectively oxidized graphene with improved electrical performance. Nanoscale, 2017, 9, 1699-1708.	5.6	49
40	Rational design of exfoliated 1T MoS ₂ @CNT-based bifunctional separators for lithium sulfur batteries. Journal of Materials Chemistry A, 2017, 5, 23909-23918.	10.3	111
41	Chemically fluorinated graphene oxide for room temperature ammonia detection at ppb levels. Journal of Materials Chemistry A, 2017, 5, 19116-19125.	10.3	83
42	Morphochemical imprinting of melamine cyanurate mesocrystals in glucose-derived carbon for high performance lithium ion batteries. Journal of Materials Chemistry A, 2017, 5, 20635-20642.	10.3	31
43	Flexible and Robust Thermoelectric Generators Based on All-Carbon Nanotube Yarn without Metal Electrodes. ACS Nano, 2017, 11, 7608-7614.	14.6	191
44	Chemical modification of graphene oxide through poly(ethylene oxide)-conjugations. Macromolecular Research, 2017, 25, 452-460.	2.4	3
45	Guidelines for Tailored Chemical Functionalization of Graphene. Chemistry of Materials, 2017, 29, 307-318.	6.7	36
46	Carbon nanosheets by the graphenization of ungraphitizable isotropic pitch molecules. Carbon, 2017, 121, 479-489.	10.3	27
47	Easy preparation of partially-opened carbon nanotubes by simple air oxidation for high performance Li–S batteries. RSC Advances, 2016, 6, 113522-113526.	3.6	8
48	Size-engineered biocompatible polymeric nanophotosensitizer for locoregional photodynamic therapy of cancer. Colloids and Surfaces B: Biointerfaces, 2016, 144, 303-310.	5.0	11
49	Titration Method for the Identification of Surface Functional Groups. , 2016, , 273-286.		7
50	High-strength carbon nanotube/carbon composite fibers via chemical vapor infiltration. Nanoscale, 2016, 8, 18972-18979.	5.6	46
51	One step preparation and excellent performance of CNT yarn based flexible micro lithium ion batteries. Energy Storage Materials, 2016, 5, 1-7.	18.0	34
52	Highâ€Performance Thermoelectric Paper Based on Double Carrierâ€Filtering Processes at Nanowire Heterojunctions. Advanced Energy Materials, 2016, 6, 1502181.	19.5	157
53	Preparation and Exceptional Mechanical Properties of Bone-Mimicking Size-Tuned Graphene Oxide@Carbon Nanotube Hybrid Paper. ACS Nano, 2016, 10, 2184-2192.	14.6	62
54	Carbon science in 2016: Status, challenges and perspectives. Carbon, 2016, 98, 708-732.	10.3	261

#	Article	IF	CITATIONS
55	Bio-inspired graphene foam decorated with Pt nanoparticles for hydrogen storage at room temperature. International Journal of Hydrogen Energy, 2016, 41, 5019-5027.	7.1	27
56	Hidden Second Oxidation Step of Hummers Method. Chemistry of Materials, 2016, 28, 756-764.	6.7	187
57	Partially unzipped carbon nanotubes for high-rate and stable lithium–sulfur batteries. Journal of Materials Chemistry A, 2016, 4, 819-826.	10.3	76
58	One-pot titration methodology for the characterization of surface acidic groups on functionalized carbon nanotubes. Carbon, 2016, 96, 729-741.	10.3	17
59	Stabilization of Insoluble Discharge Products by Facile Aniline Modification for High Performance Liâ€ S Batteries. Advanced Energy Materials, 2015, 5, 1500268.	19.5	51
60	The influence of microstructure of carbon nanotubes on the degree of length reduction during melt processing with polycarbonate. , 2015, , .		0
61	Wrapping SnO2 with porosity-tuned graphene as a strategy for high-rate performance in lithium battery anodes. Carbon, 2015, 85, 289-298.	10.3	51
62	Highly Reproducible Thermocontrolled Electrospun Fiber Based Organic Photovoltaic Devices. ACS Applied Materials & Interfaces, 2015, 7, 4481-4487.	8.0	18
63	The effect of surface characteristics of reduced graphene oxide on the performance of a pseudocapacitor. 2D Materials, 2015, 2, 014007.	4.4	18
64	Effect of microstructure and morphological properties of carbon nanotubes on the length reduction during melt processing. Composites Science and Technology, 2015, 112, 42-49.	7.8	9
65	Effect of polymer infiltration on structure and properties of carbon nanotube yarns. Carbon, 2015, 88, 60-69.	10.3	105
66	Role of oxygen functional groups in graphene oxide for reversible room-temperature NO2 sensing. Carbon, 2015, 91, 178-187.	10.3	183
67	Remarkable Conversion Between n- and p-Type Reduced Graphene Oxide on Varying the Thermal Annealing Temperature. Chemistry of Materials, 2015, 27, 7362-7369.	6.7	177
68	Easy Preparation of Self-Assembled High-Density Buckypaper with Enhanced Mechanical Properties. Nano Letters, 2015, 15, 190-197.	9.1	69
69	New insights into the oxidation of single-walled carbon nanotubes for the fabrication of transparent conductive films. Carbon, 2015, 81, 525-534.	10.3	16
70	Effect of annealing with pressure on tungsten film properties fabricated by atmospheric plasma spray. Metals and Materials International, 2014, 20, 1037-1042.	3.4	14
71	Effects of chirality and diameter of single-walled carbon nanotubes on their structural stability and solubility parameters. RSC Advances, 2014, 4, 33578.	3.6	3
72	Unusual thermopower of inhomogeneous graphene grown by chemical vapor deposition. Applied Physics Letters, 2014, 104, 021902.	3.3	13

#	Article	IF	CITATIONS
73	Theoretical guidelines to designing high performance energy storage device based on hybridization of lithium-ion battery and supercapacitor. Journal of Power Sources, 2014, 259, 1-14.	7.8	62
74	One step synthesis of sulfur–carbon nanosheet hybrids via a solid solvothermal reaction for lithium sulfur batteries. RSC Advances, 2014, 4, 3684-3690.	3.6	11
75	Enhanced water stability and CO ₂ gas sorption properties of a methyl functionalized titanium metal–organic framework. New Journal of Chemistry, 2014, 38, 2752-2755.	2.8	19
76	Preparation of PCDTBT nanofibers with a diameter of 20 nm and their application to air-processed organic solar cells. Nanoscale, 2014, 6, 2847.	5.6	26
77	Experimental consideration of the Hansen solubility parameters of as-produced multi-walled carbon nanotubes by inverse gas chromatography. Physical Chemistry Chemical Physics, 2014, 16, 17466.	2.8	32
78	Easy Preparation of Readily Self-Assembled High-Performance Graphene Oxide Fibers. Chemistry of Materials, 2014, 26, 5549-5555.	6.7	52
79	Facile preparation of reduced graphene oxide-based gas barrier films for organic photovoltaic devices. Energy and Environmental Science, 2014, 7, 3403-3411.	30.8	58
80	Solvent evaporation mediated preparation of hierarchically porous metal organic framework-derived carbon with controllable and accessible large-scale porosity. Carbon, 2014, 71, 294-302.	10.3	77
81	Conjugated Polymer/Photochromophore Binary Nanococktails: Bistable Photoswitching of Nearâ€Infrared Fluorescence for In Vivo Imaging. Advanced Materials, 2013, 25, 5574-5580.	21.0	55
82	Water-Soluble Fluorinated and PEGylated Cyanostilbene Derivative: An Amphiphilic Building Block Forming Self-Assembled Organic Nanorods with Enhanced Fluorescence Emission. Chemistry of Materials, 2013, 25, 3288-3295.	6.7	58
83	Effect of Helmholtz Oscillation on Auto-shroud for APS Tungsten Carbide Coating. Journal of Thermal Spray Technology, 2013, 22, 756-763.	3.1	1
84	Preparation of a freestanding, macroporous reduced graphene oxide film as an efficient and recyclable sorbent for oils and organic solvents. Journal of Materials Chemistry A, 2013, 1, 9427.	10.3	80
85	Determination of solubility parameters of single-walled and double-walled carbon nanotubes using a finite-length model. RSC Advances, 2013, 3, 4814.	3.6	30
86	Poly(oxyethylene sugaramide)s: unprecedented multihydroxyl building blocks for tumor-homing nanoassembly. Journal of Materials Chemistry B, 2013, 1, 3437.	5.8	2
87	The effect of heating rate on porosity production during the low temperature reduction of graphite oxide. Carbon, 2013, 53, 73-80.	10.3	59
88	Ultrafast room-temperature reduction of graphene oxide to graphene with excellent dispersibility by lithium naphthalenide. Carbon, 2013, 63, 165-174.	10.3	23
89	Preparation and Exceptional Lithium Anodic Performance of Porous Carbon-Coated ZnO Quantum Dots Derived from a Metal–Organic Framework. Journal of the American Chemical Society, 2013, 135, 7394-7397.	13.7	482
90	Effect of solvents and thermal annealing on the morphology development of a novel block copolymer ionomer: a case study of sulfonated polystyrene-block-fluorinated polyisoprene. Journal of Polymer Engineering, 2013, 33, 49-59.	1.4	3

#	Article	IF	CITATIONS
91	Quantum Hall effect in graphene decorated with disordered multilayer patches. Applied Physics Letters, 2013, 103, .	3.3	39
92	Effect of solvents and thermal annealing on the morphology development of a novel block copolymer ionomer: a case study of sulfonated polystyrene-block-fluorinated polyisoprene; J. Polym. Eng. 2013, 33, 49–59. Journal of Polymer Engineering, 2013, 33, 191-191.	1.4	1
93	Effects of morphological characteristics of Pt nanoparticles supported on poly(acrylic acid)-wrapped multiwalled carbon nanotubes on electrochemical performance of direct methanol fuel cells. Journal of Materials Research, 2012, 27, 2035-2045.	2.6	6
94	Advanced energy storage device: a hybrid BatCap system consisting of battery–supercapacitor hybrid electrodes based on Li4Ti5O12–activated-carbon hybrid nanotubes. Journal of Materials Chemistry, 2012, 22, 16986.	6.7	117
95	Influence of H+ ion irradiation on the surface and microstructural changes of a nuclear graphite. Fusion Engineering and Design, 2012, 87, 344-351.	1.9	25
96	Recent advances in hydrogen storage technologies based on nanoporous carbon materials. Progress in Natural Science: Materials International, 2012, 22, 631-638.	4.4	80
97	General Relationship between Hydrogen Adsorption Capacities at 77 and 298 K and Pore Characteristics of the Porous Adsorbents. Journal of Physical Chemistry C, 2012, 116, 10529-10540.	3.1	50
98	Simple fabrication of carbon/TiO ₂ composite nanotubes showing dual functions with adsorption and photocatalytic decomposition of Rhodamine B. Nanotechnology, 2012, 23, 035604.	2.6	45
99	MOF-Derived Hierarchically Porous Carbon with Exceptional Porosity and Hydrogen Storage Capacity. Chemistry of Materials, 2012, 24, 464-470.	6.7	671
100	Preparation of Highly Moistureâ€Resistant Blackâ€Colored Metal Organic Frameworks. Advanced Materials, 2012, 24, 4010-4013.	21.0	166
101	Surface modifications for the effective dispersion of carbon nanotubes in solvents and polymers. Carbon, 2012, 50, 3-33.	10.3	608
102	Simple and cost-effective reduction of graphite oxide by sulfuric acid. Carbon, 2012, 50, 3229-3232.	10.3	70
103	Effects of carbon dioxide and acidic carbon compounds on the analysis of Boehm titration curves. Carbon, 2012, 50, 1510-1516.	10.3	33
104	A simple method for determining the neutralization point in Boehm titration regardless of the CO2 effect. Carbon, 2012, 50, 3315-3323.	10.3	41
105	Effects of structural modifications on the hydrogen storage capacity of MOF-5. International Journal of Hydrogen Energy, 2012, 37, 5777-5783.	7.1	31
106	Preparation and photoluminescence (PL) performance of a nanoweb of P3HT nanofibers with diameters below 100 nm. Journal of Materials Chemistry, 2011, 21, 14231.	6.7	39
107	Preparation and electrochemical performance of hyper-networked Li4Ti5O12/carbon hybrid nanofiber sheets for a battery–supercapacitor hybrid system. Nanotechnology, 2011, 22, 405402.	2.6	53
108	Si-doping effect on the enhanced hydrogen storage of single walled carbon nanotubes and graphene. International Journal of Hydrogen Energy, 2011, 36, 12286-12295.	7.1	87

#	Article	IF	CITATIONS
109	Oxidative stabilization of conjugated linoleic acid by one-pot PEGylation. Macromolecular Research, 2011, 19, 822-826.	2.4	1
110	MOF-derived ZnO and ZnO@C composites with high photocatalytic activity and adsorption capacity. Journal of Hazardous Materials, 2011, 186, 376-382.	12.4	116
111	Enhanced hydrogen storage capacity of Pt-loaded CNT@MOF-5 hybrid composites. International Journal of Hydrogen Energy, 2010, 35, 13062-13067.	7.1	100
112	Effects of surrounding confinements of Si nanoparticles on Si-based anode performance for lithium ion batteries. Electrochimica Acta, 2010, 56, 790-796.	5.2	49
113	Concentration-Driven Evolution of Crystal Structure, Pore Characteristics, and Hydrogen Storage Capacity of Metal Organic Framework-5s: Experimental and Computational Studies. Chemistry of Materials, 2010, 22, 6138-6145.	6.7	18
114	Effect of multi-walled carbon nanotube dispersion on the electrical, morphological and rheological properties of polycarbonate/multi-walled carbon nanotube composites. Macromolecular Research, 2009, 17, 863-869.	2.4	58
115	Easy synthesis of highly nitrogen-enriched graphitic carbon with a high hydrogen storage capacity at room temperature. Carbon, 2009, 47, 1585-1591.	10.3	102
116	Catalyst-free and template-free preparation of semi-cylindrical carbon nanoribbons. Carbon, 2009, 47, 2391-2395.	10.3	5
117	A simple and highly effective process for the purification of single-walled carbon nanotubes synthesized with arc-discharge. Carbon, 2009, 47, 3544-3549.	10.3	28
118	Preparation and Enhanced Hydrostability and Hydrogen Storage Capacity of CNT@MOF-5 Hybrid Composite. Chemistry of Materials, 2009, 21, 1893-1897.	6.7	336
119	Regioselective succinylation and gelation behavior of glycol chitosan. Macromolecular Research, 2008, 16, 57-61.	2.4	10
120	Dual functions of ferrous sulfate as a pore-size controller and a carbon-yield enhancer in fabricating cellulose based porous carbons. Fibers and Polymers, 2008, 9, 160-165.	2.1	0
121	Facile preparation of monodisperse ZnO quantum dots with high quality photoluminescence characteristics. Nanotechnology, 2008, 19, 035609.	2.6	44
122	Highly fluorescent columnar liquid crystals with elliptical molecular shape: oblique molecular stacking and excited-state intramolecular proton-transfer fluorescence. Journal of Materials Chemistry, 2007, 17, 5052.	6.7	67
123	Controlled assembly of carbon nanotubes encapsulated with amphiphilic block copolymer. Carbon, 2007, 45, 2072-2078.	10.3	28
124	Hydrogen storage on Li-doped single-walled carbon nanotubes: Computer simulation using the density functional theory. Catalysis Today, 2007, 120, 407-412.	4.4	42
125	The enhanced anodic performance of highly crimped and crystalline nanofibrillar carbon in lithium-ion batteries. Electrochimica Acta, 2007, 53, 944-950.	5.2	6
126	Compressional behavior of carbon nanotube reinforced mesophase pitch-based carbon fibers. Fibers and Polymers, 2006, 7, 85-87.	2.1	13

#	Article	IF	CITATIONS
127	Accurate measurement of interlayer spacing value of carbon fibers using a silver foil as an internal standard. Carbon, 2006, 44, 1016-1019.	10.3	6
128	Preparation and characterization of self-assembled nanoparticles based on glycol chitosan bearing adriamycin. Colloid and Polymer Science, 2006, 284, 763-770.	2.1	47
129	Preparation and characterization of cisplatin-incorporated chitosan hydrogels, microparticles, and nanoparticles. Macromolecular Research, 2006, 14, 573-578.	2.4	34
130	Effects of sulfuric acid treatment on the microstructure and electrochemical performance of a polyacrylonitrile (PAN)-based carbon anode. Carbon, 2005, 43, 163-169.	10.3	48
131	Nanofibril Formation of Electrospun TiO2Fibers and its Application to Dyeâ€Sensitized Solar Cells. Journal of Macromolecular Science - Pure and Applied Chemistry, 2005, 42, 1529-1540.	2.2	43
132	Specification for a standard procedure of X-ray diffraction measurements on carbon materials. Carbon, 2004, 42, 701-714.	10.3	414
133	Biodistribution and anti-tumor efficacy of doxorubicin loaded glycol-chitosan nanoaggregates by EPR effect. Journal of Controlled Release, 2003, 91, 135-145.	9.9	266
134	Contribution of inorganic components in precursors to porosity evolution in biomass-based porous carbons. Carbon, 2003, 41, 2009-2012.	10.3	31
135	Analysis of Problematic Complexing Behavior of Ferric Chloride withN,N-Dimethylformamide Using Combined Techniques of FT-IR, XPS, and TGA/DTG. Inorganic Chemistry, 2002, 41, 6211-6216.	4.0	109
136	Preparation and characteristics of rice-straw-based porous carbons with high adsorption capacity. Fuel, 2002, 81, 327-336.	6.4	191
137	Structural Characteristics of Size-Controlled Self-Aggregates of Deoxycholic Acid-Modified Chitosan and Their Application as a DNA Delivery Carrier. Bioconjugate Chemistry, 2001, 12, 932-938.	3.6	200
138	Syntheses of new film-forming aromatic poly(amide-imide)s containing isoindoloquinazolinedione unit in the backbone: Poly(biphenylphthalicdianhydride-oxydianiline-4,4′-diamino-3′-carbamoyl-benzanilide) (poly(BPDA-ODA-DACB)). Fibers and Polymers, 2001, 2, 92-97.	2.1	1
139	Synthesis and polymerization mechanism of bisacetoacetamides. Journal of Polymer Science Part A, 2001, 39, 1456-1462.	2.3	5
140	Effects of pre-carbonization on porosity development of activated carbons from rice straw. Carbon, 2001, 39, 559-567.	10.3	106
141	Preparation and properties of activated carbon fabric from acrylic fabric waste. Carbon, 2000, 38, 1453-1460.	10.3	37
142	Preparation and Solubility in Acid and Water of Partially Deacetylated Chitins. Biomacromolecules, 2000, 1, 609-614.	5.4	199
143	Monte Carlo simulation of copolymerization by ester interchange reaction in miscible polyester blends. Journal of Polymer Science, Part B: Polymer Physics, 1998, 36, 1637-1645.	2.1	15
144	Preparation of poly(ethylene terephthalate-co-isophthalate) by ester interchange reaction in the PET/PEI blend system. Journal of Polymer Science, Part B: Polymer Physics, 1997, 35, 309-315.	2.1	32

#	Article	IF	CITATIONS
145	New modified poly(ethylene terephthalate) (MPET)-based adsorbent for heavy metal ions. Journal of Applied Polymer Science, 1997, 63, 773-778.	2.6	14
146	Effect of chemical structure on crystallization behavior of poly(phenylene alkylene dicarboxylate) (PPAD). Journal of Applied Polymer Science, 1997, 66, 1575-1582.	2.6	2
147	Compressional behaviour of carbon fibres. Journal of Materials Science, 1990, 25, 829-834.	3.7	65